

THE USE OF THERMAL HYDROGEN DECREPITATION TO RECYCLE Nd-Fe-B  
MAGNETS FROM ELECTRONIC WASTEA. Piotrowicz <sup>a,\*</sup>, S. Pietrzyk <sup>b</sup>, P. Noga <sup>a</sup>, L. Myćka <sup>a</sup><sup>a</sup> AGH University of Science and Technology, Faculty of Non-Ferrous Metals, Cracow, Poland<sup>b</sup> Łukasiewicz Research Network - Institute of Non-Ferrous Metals, Gliwice, Poland

(Received 07 February 2020; Accepted 12 november 2020)

**Abstract**

Rare earth magnets based upon neodymium-iron-boron (NdFeB) are employed in many high tech applications, including hard disk drives (HDDs). The key elements in manufacturing NdFeB magnets are rare earth elements (REEs) such as neodymium. This element has been subject to significant supply shortfalls in the recent past. Recycling of NdFeB magnets contained within waste of electrical and electronic equipment (WEEE) could provide a secure and alternative supply of these materials. Various recycling approaches for the recovery of sintered NdFeB magnets have been widely explored. Hydrogen decrepitation (HD) can be used as a direct reuse approach and effective method of recycling process to turn solid sintered magnets into a demagnetised powder for further processing. In this work, sintered Nd-Fe-B magnets were processed without prior removal of the metallic protective layer using the thermal HD process as an alternative recycling method. The gas sorption analyzer was used to determine the quantity of the hydrogen absorbed by a samples of magnets, under controlled pressure (1, 2, 3, and 4 bar) and temperature (room, 100, 300, and 400 °C) conditions, using Sieverts' volumetric method. The composition and morphology of the starting and the extracted/disintegrated materials were examined by ICP, XRD, and SEM-EDS analysis.

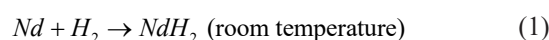
**Keywords:** Neodymium magnet; NdFeB recycling; Hydrogen decrepitation**1. Introduction**

There are several pyro- and hydrometallurgical methods of Nd-Fe-B magnets recycling by: oxidation [1-3] or chlorination [1, 2, 5, 4], extraction from liquid phase using magnesium [6, 7], electrolysis in molten salts [1, 7-11], reduction-diffusion route method using calcium [12], and hydrogen decrepitation [1, 13-19]. Many of these are under current development.

Hydrogen decrepitation (HD) is based on the selective synthesis of neodymium hydrides though the reaction of hydrogen gas with neodymium located in the Nd-Fe-B magnet. HD process was originally designed and patented by Harris et al. (1979) as a way to break down  $\text{SmCo}_5$  and  $\text{Sm}_2(\text{Co,Fe,Cu,Zr})_{17}$  alloys. It was subsequently modified by Harris et al. (1985) to disintegrate the newly developed NdFeB alloy. During the HD process, NdFeB alloy is usually exposed to hydrogen and the hydrogenation process causes a volume expansion by 5 %, which promotes the formation of intergranular and transboundary cracks, and this in turn causes the crushing of the material. The volume increase takes place in the whole volume of the magnet, causing disintegration to form bulks or powder [13-18].

During the HD process, various phase changes occur in the magnet microstructure (Figure 1). Due to the composition of the magnet, two types of reaction are distinguished [16]:

between hydrogen and Nd-rich phase:



between hydrogen and  $\text{NdH}_2\text{Fe}_{14}\text{B}$  phase (disproportionation):

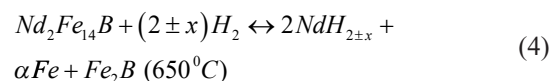
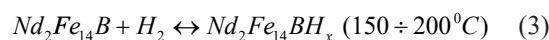


Illustration A in Figure 1 shows the initial  $\text{Nd}_2\text{Fe}_{14}\text{B}$  microstructure scheme. During the HD process, reactions occur along the grain boundaries and at the triple points (B in Figure 1), because these are the preferred areas from the kinetic point of view. Depending on the process temperature, reaction 1 or/and 2 occur. Then, hydrogenation and

\*Corresponding author: andpio@agh.edu.pl



disproportionation (reactions 3 and 4) are initiated along the grain boundary and at triple points (C in Figure 1). At triple points there is  $\text{NdH}_2$  in the iron matrix with finely dispersed  $\text{Fe}_2\text{B}$ . Disproportionation spreads to the interior of the  $\text{Nd}_2\text{Fe}_{14}\text{B}$  phase, creating so-called pools (extensive areas to the origin of the triple points or unreacted Nd-rich areas) and connecting their necks, i.e. grain boundaries consisting of neodymium hydrides, until finally they cover the entire magnet [13-18].

An important parameter of the decrepitation process is temperature. With increasing temperature, free enthalpy value of  $\text{NdH}_2$  formation increases, therefore the spontaneity of the synthesis reaction decreases. For this reason, the process temperature indirectly affects the size of the particle obtained after hydrogenation: the higher the temperature, the larger the grains of disintegrated material [13].

Due to the fact that neodymium magnets are often covered with a protective coating (metallic or plastic) that protects the magnet against corrosion, in recycling is important to separate it from the magnet. Decrepitation allows this separation, if the following conditions are met:

- magnets contain protective coating that is not damaged; otherwise it is possible that the components of the magnet scrap will react with oxygen or moisture that prevents the synthesis of hydrides, and thus the decrepitation process;
- hydrogen diffuses through the protective coating, which may require a long duration due to e.g. hydrogen sorption by nickel, which is often included in the coating;
- a fine neodymium magnet powder and pieces of protective coating are formed, which can be easily separated by sieving.

For example, the separation of the protective

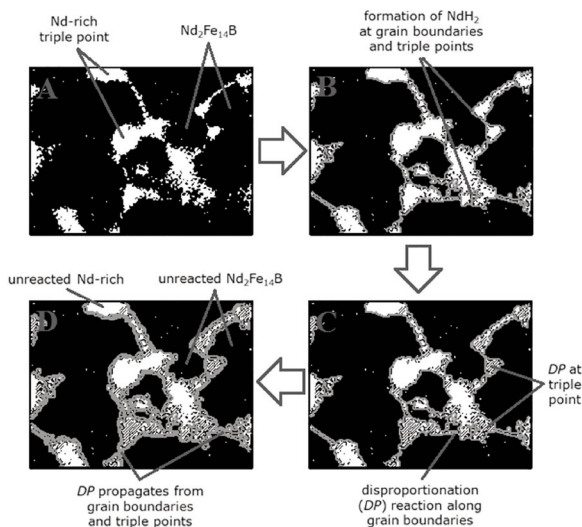


Figure 1. Changes in the microstructure of Nd-Fe-B magnet in the HD process

coating can be carried out by sieving (90  $\mu\text{m}$ ), which results in a decreasing of the nickel content to 400 ppm [18].

The decrepitation process can be an integral part of the neodymium magnet manufacturing process [15, 20, 21]. The hydrogenated material can be used in various ways: as a neodymium-rich concentrate or as an initial material for the manufacturing of new magnets.

## 2. Experimental

The aim of this work was to examine the recycling process of Nd-Fe-B magnets using HD process and to determine the optimal technological parameters: temperature and pressure. The influence of parameters was determined by examining morphology and phases changes after decrepitation. The possibility of separation the protective coating from the disintegrated magnet by sieving was also tested.

The study was conducted in the following order:

- characteristics of the initial material,
- demagnetization,
- hydrogenation/disintegration,
- characteristics of the disintegrated material, and
- sieving tests.

The initial material was commercial cuboids neodymium magnets Nd-Fe-B N42 with dimensions of 25x10x2 mm covered with a metallic protective coating. The composition of the initial material was examined by ICP-MS method on an ELAN 6100 analyzer (Perkin Elmer); sample (demagnetized and crushed magnet with coating) was dissolved in hot aqua regia and examined for composition. Before the hydrogenation process, the magnets were demagnetized at 350  $^{\circ}\text{C}$  (above the Curie point) for 1 h in a slightly oxidizing atmosphere. Hydrogenation (i.e. hydrogen sorption) of neodymium magnets was carried out using the gas sorption analyzer IMI-0118 (Hiden Isochema), whose operation is based on the Sievert volumetric method. To determine the phase changes after HD, magnets were examined by x-ray powder diffraction method on a Rigaku MiniFlex II. Morphological changes were determined by analysis on a scanning electron microscope Hitachi SU 70. The separation possibility of magnet from coating was tested by sieving of disintegrated magnets on a metallic sieve with a 3 mm square mesh.

## 3. Results and discussion

The chemical composition of the initial material is shown in Table 1. In addition to the typical composition of neodymium magnets (Fe, Nd, and B), the initial material contained small amounts of dysprosium (0.12 wt.%), as well as nickel, copper and cobalt (in total about 3.95 wt.%), which come from a



protective coating.

The composition of the protective coating was also confirmed by the cross-sectional analysis (Figure 2). The protective coating was compact, had a thickness of approx. 13 μm. Interior of the magnet (i.e. away of the coating) had a typical neodymium magnet composition.

As a result of demagnetization in slightly oxidizing atmosphere, the protective coating oxidized, which was deduced after the color coating changed (Figure 3). The disintegration was estimated arbitrary based on the appearance of the samples after decrepitation process, i.e. whether the sample completely disintegrated into powder and whether the protective coating was detached from the magnet. Based on subsequent photos (Figure 3), it can be concluded that the magnets exposed to hydrogen atmosphere at 29 and 100 °C were completely disintegrated. Other samples were only partially or slightly disintegrated. The least disintegration was observed in magnets exposed to hydrogen atmosphere at 400 °C at 1 and 2 bar pressure. These samples disintegrated into large pieces, from which the protective coating did not detached. In cases of well disintegrated samples, it was easy to see the peeled off

layers of the protective coating.

The results from the hydrogen sorption analyzer (Tables 2 and 3) show that the highest hydrogen uptake (2043.76 μmol·g<sup>-1</sup>) was received for conditions 4 bar and room temperature, while the lowest (925.27 μmol·g<sup>-1</sup>) for 1 bar at 400 °C (Figure 4). At room temperature (29 °C), hydrogen uptake increased (from 1853.85 to 2043.76 μmol·g<sup>-1</sup>) with increasing pressure and with decreasing process duration (from 869 min to 228 min) from 2 to 4 bar, respectively. An increase in temperature causes a decrease in the hydrogen uptake value. Maximum uptake values received at 300 and 400 °C were almost two times lower than maximum uptake values at room temperature and 4 bar conditions.

Morphological differences that occurred in the hydrogenated samples, in relation to the initial material, are shown in Figures 5-7. The initial material (A in Figure 5) consisted of evenly distributed regular grains with different chemical composition: in microscopic images, bright areas indicated higher content of neodymium, while dark -

**Table 1.** Chemical composition of the initial material examined by ICP-MS

wt.%	Nd	Fe	B	Dy	Ni	Cu	Co	other
	7.77	83.98	2.14	0.12	0.85	2.15	0.95	2.04

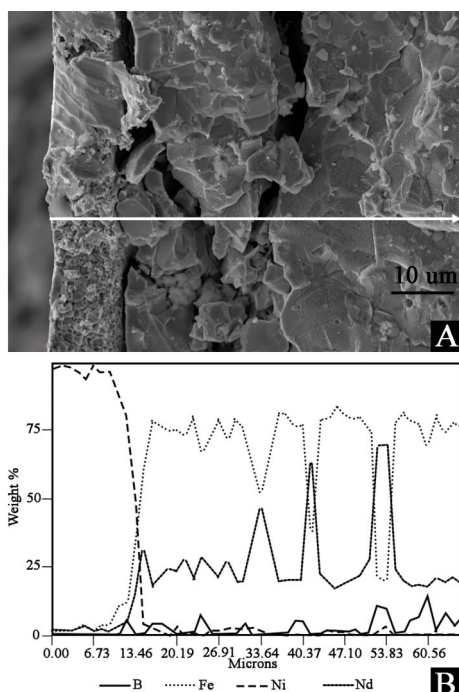


**Figure 2.** SEM-EDS analyses of the magnet with protective coating: A - SEM image of a cross-section, B - EDS cross-sectional analysis



**Figure 3.** Initial, demagnetized and disintegrated magnets; dark grey captions indicates those samples which are indicated as fully disintegrated

**Table 2.** Maximum hydrogen uptakes (μmol·g<sup>-1</sup>) vs temperature and pressure

		temperature (°C)			
		29	100	300	400
pressure (bar)	1	-	1569.58	1107.16	925.27
	2	1853.86	-	1131.42	1230.6
	3	2007.31	-	-	-
	4	2043.76	-	-	-

**Table 3.** Decrepitation duration (min) vs temperature and pressure

		temperature (°C)			
		29	100	300	400
pressure (bar)	1	-	540	623	279
	2	869	-	243	205
	3	272	-	-	-
	4	228	-	-	-



iron; this was also confirmed by mapping. In samples received at 2 bar at 300 and 400 °C (respectively B and C in Figure 5) homogenization of the composition occurred: microscopic images have less contrast (they are brighter) and mapping showed even distributions of neodymium and iron, which is clearly shown in B in Figure 5. Homogenization could be promoted by high temperature. The situation is different in the case

of the samples gained at 1 bar in different temperatures (D, E and F, in Figure 6): on mapping it can be seen specific necks and pools, which were rich in neodymium, resulting from the synthesis of neodymium hydrides. Areas where neodymium occurs were also poor in iron. Despite successful disintegration, the large grains with sizes that correspond to grains in the initial material can still

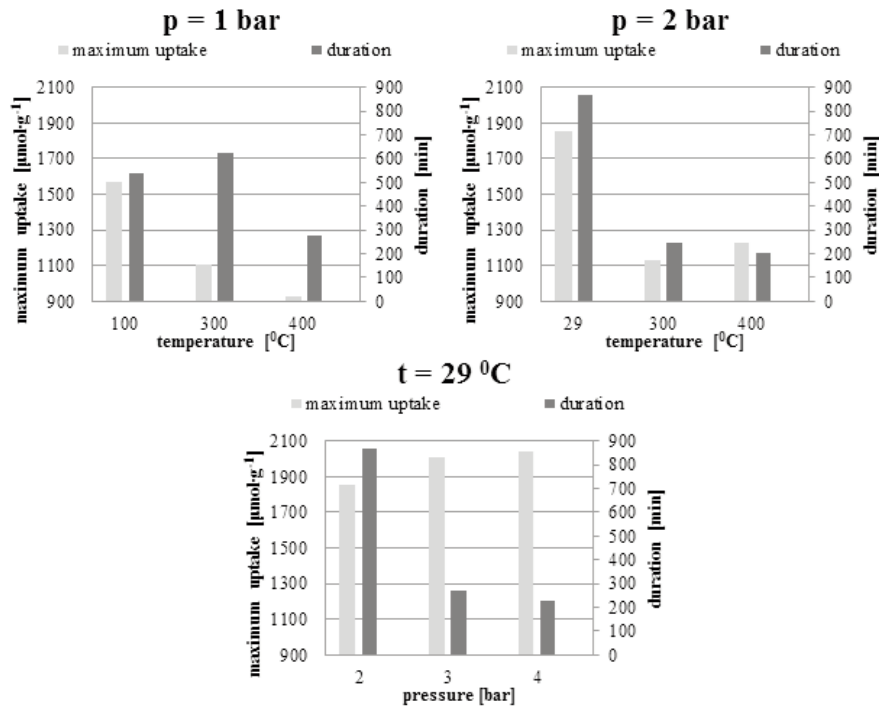


Figure 4. Relationships between maximum hydrogen uptakes and decrepitation duration vs temperature at 1 bar (left) and 2 bar (middle) and vs pressure at room temperature (right)

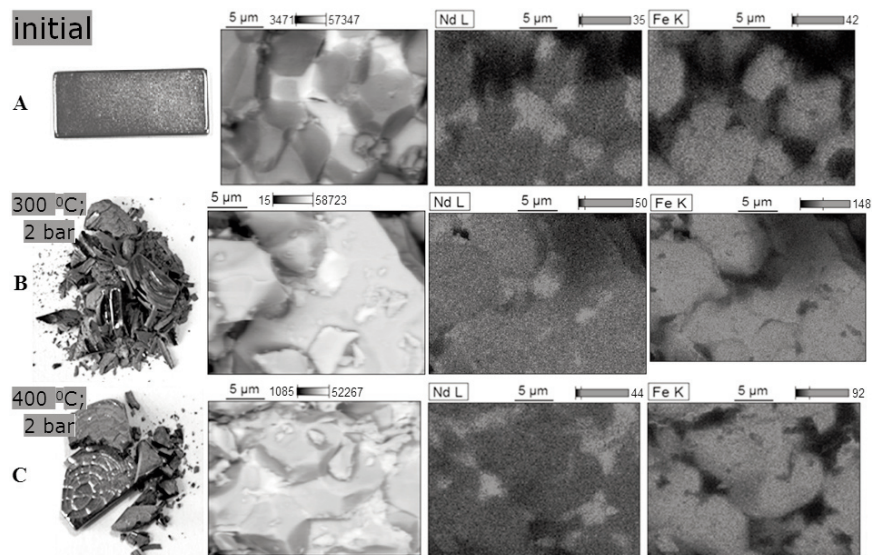


Figure 5. SEM and mapping analyses of the initial material (A) and samples after decrepitation at following conditions: 300 °C and 2 bar (B), 400 °C and 2 bar (C)

distinguished in the disintegrated material. As mentioned earlier, samples that were decrepitated at room temperature (G, H, and I in Figure 7) had the highest maximum uptake values. While in the samples gained at 2 and 3 bar (G and H in Figure 7) grains of the size corresponding to the initial material can be distinguished, in the case of the sample gained at 4 bar (I) material disintegrated into a finer powder. In samples H and I it was difficult to distinguish the necks, but it was easier to observe the pools, which may indicate that the hydrides synthesis reactions took place to a large extent.

Phase changes of the magnets after decrepitation

were presented in XRD spectrograms (Figures 8-16). Most probably, the reflections at 50 and 52 deg are due to the presence of the  $\alpha$ -Fe phase, but were not included; only phases containing neodymium were marked in spectrograms. The XRD pattern of the initial material (Figure 8) consisted only of the reflections from the  $\text{Nd}_2\text{Fe}_{14}\text{B}$  phase, while after HD, reflections from the synthesized neodymium hydrides appeared:  $\text{NdH}_2$ ,  $\text{NdH}_{2.27}$ , and  $\text{NdH}_3$ . Reflections from the following hydrides were on each spectrograms (Figures 9-16):  $\text{NdH}_2$  at approx. 28 and 69 deg,  $\text{NdH}_{2.27}$  at 28.5 deg, and  $\text{NdH}_3$  at 37.5, 57, and 60.5 deg. Furthermore, in the samples that were obtained

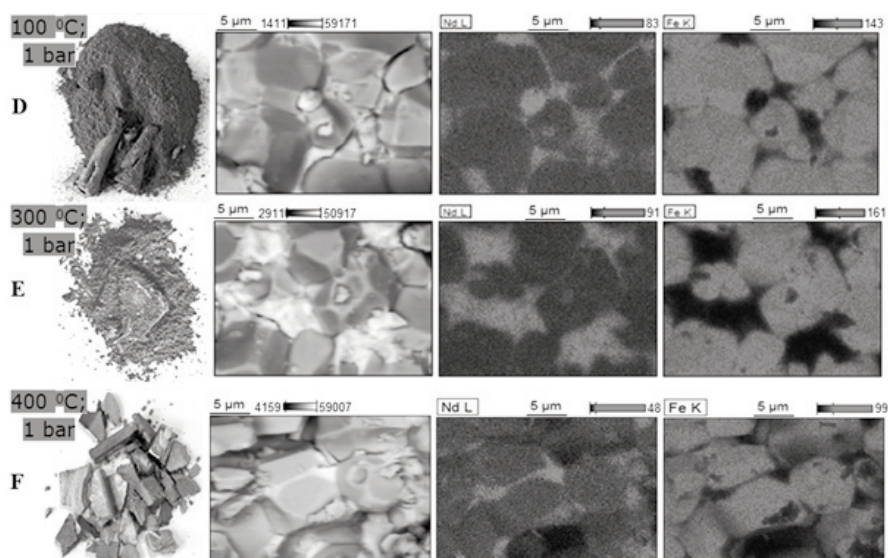


Figure 6. SEM and mapping analyses of samples after decrepitation at following conditions: 100 °C and 1 bar (D), 300 °C and 1 bar (E) and 400 °C and 1 bar (F)

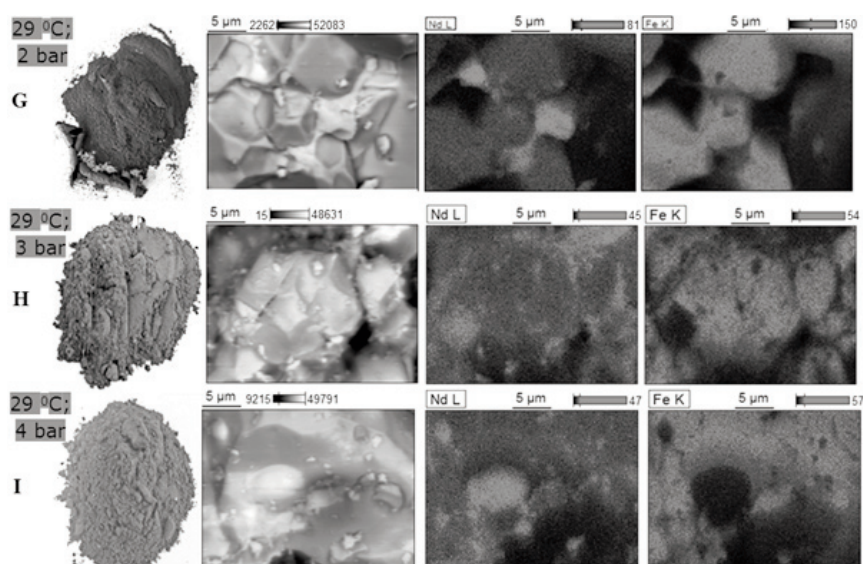


Figure 7. SEM and mapping analyses of samples after decrepitation at following conditions: room temperature and 2 bar (G), room temperature and 3 bar (H) and room temperature and 4 bar (I)

as a result of decrepitation at 100 °C (Figure 11) and room temperature and high pressure (Figures 14-16), there were additional reflections from  $\text{NdH}_{2.27}$  also at

47 and 56 deg. Hence it can be concluded that not only the temperature but also the pressure increase promoted occurring of disproportionation reactions.

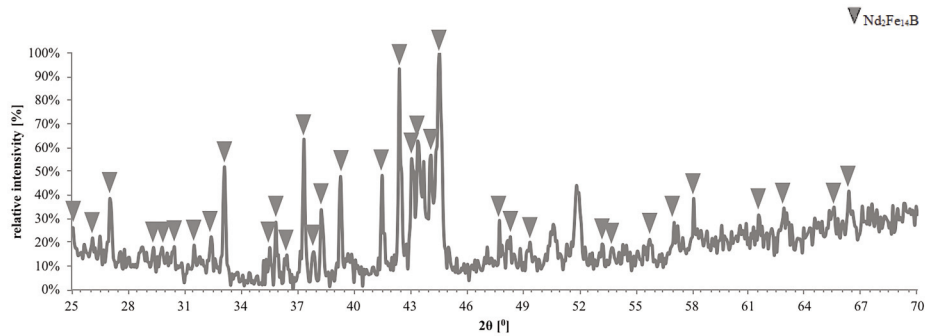


Figure 8. XRD patterns of initial material

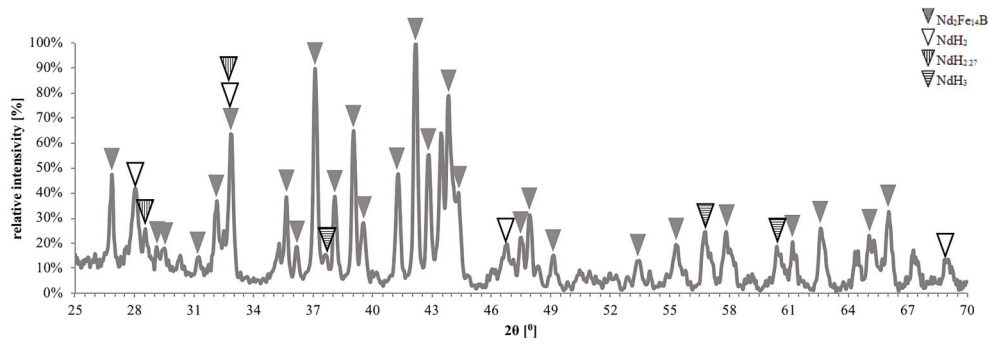


Figure 9. XRD patterns of sample obtained at 300 °C and 2 bar

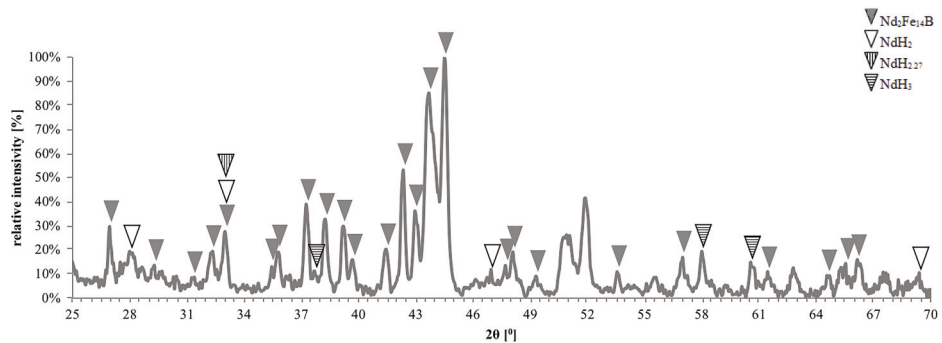


Figure 10. XRD patterns of sample obtained at 400 °C and 2 bar

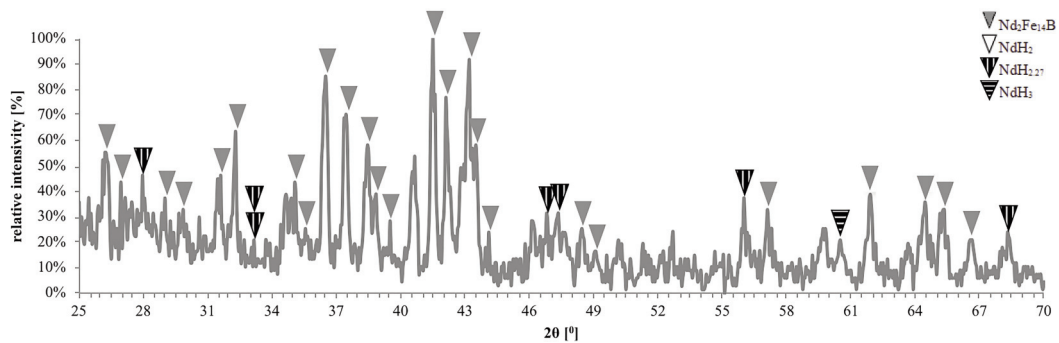


Figure 11. XRD patterns of sample obtained at 100 °C and 1 bar

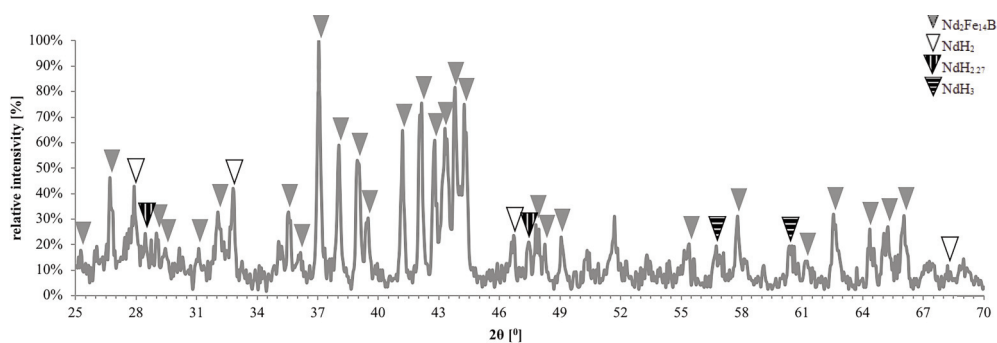


Figure 12. XRD patterns of sample obtained at 300 °C and 1 bar

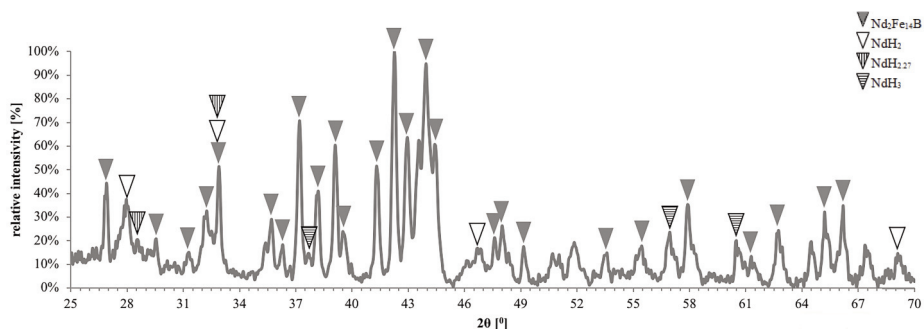


Figure 13. XRD patterns of sample obtained at 400 °C and 1 bar

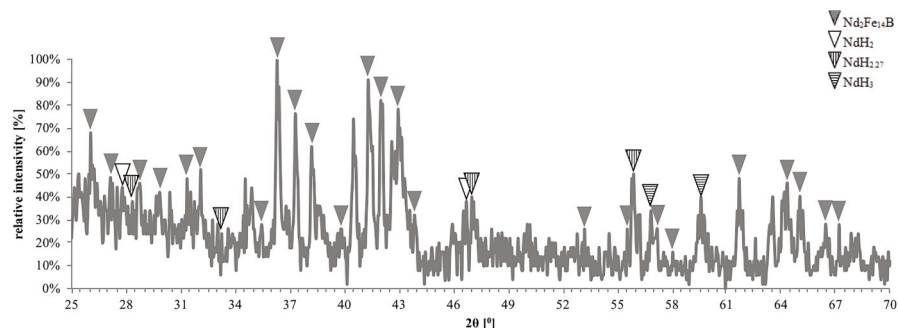


Figure 14. XRD patterns of sample obtained at room temperature and 2 bar

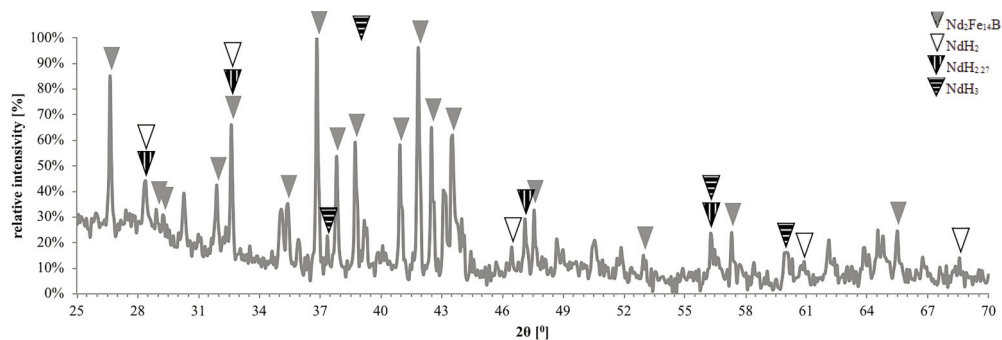


Figure 15. XRD patterns of sample obtained at room temperature and 3 bar

Sieving tests were performed on fully disintegrated samples. Results of these tests are shown in Figure 17. Best results of coating separation were gained for samples 29 °C, 2 bar and also 100 °C,

1 bar, because the separated pieces of the coating were compact and large. Despite this, in each case, small pieces of coating still remained in the samples. However, the sieving tests demonstrated that it was

possible to separate the protective coating from magnet after decrepitation, and the effectiveness of this operation depended on the chosen mesh.

Figure 18 is a presentation of SEM images of the sieved materials (under the mesh). These are fine powders, for which the average particle diameter was in the range 10.30-15.60 μm (Table 4), depending on the material. In this regard, these particles were not homogeneous, what can be derived from the values of the standard deviations (Table 4). Their chemical

composition (Table 5) was characterized by a low level of nickel (0.11-0.34 wt.%), which confirmed the effectiveness of separating the magnets after decrepitation from protective coating.

**Table 4.** Average particle diameters (and standard deviations) of the sieved material; average particle diameters based on SEM images (calculations were carried out using the ImageJ software)

		sieved material			
		29 °C; 2 bar	100 °C; 1 bar	29 °C; 3 bar	29 °C; 4 bar
Nd	wt. %	7.68	10.71	8.69	11.61
Fe		53.53	57.55	54.77	62.95
B		34.16	27.13	31.66	20.6
Ni		0.14	0.11	0.15	0.34
other		4.49	4.5	4.73	4.5

**Table 5.** Chemical composition of the sieved material examined by ICP-MS (without hydrogen)

	sieved material			
	29 °C; 2 bar	100 °C; 1 bar	29 °C; 3 bar	29 °C; 4 bar
average particle diameter (μm)	14.75	15.6	11.3	12.29
standard deviation of average particle diameter (μm)	7.11	5.42	4.35	5.37

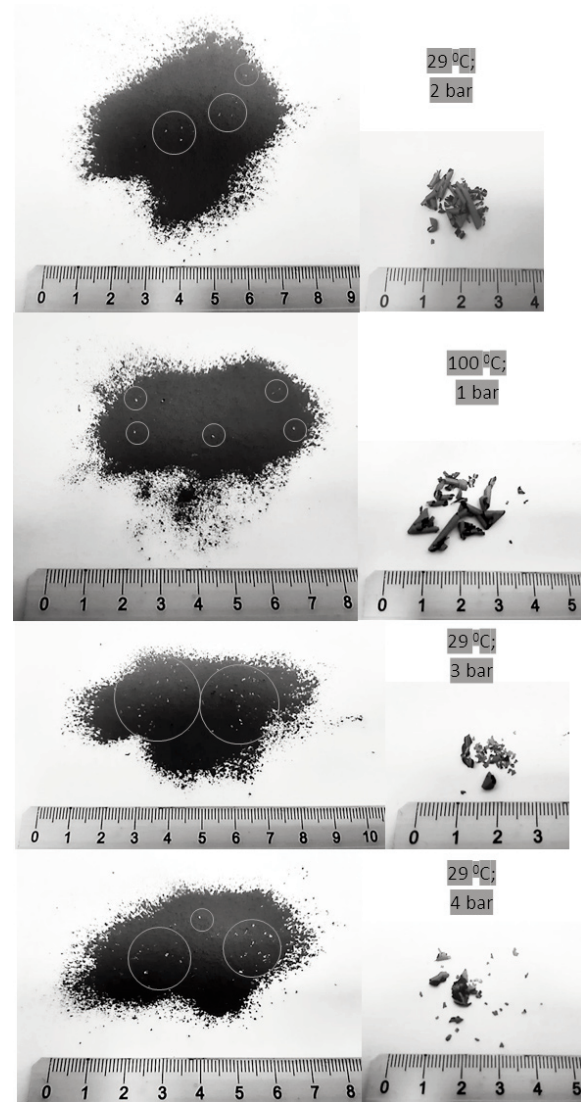


**Figure 17.** Results of sieving tests; the coating flakes are marked with circles

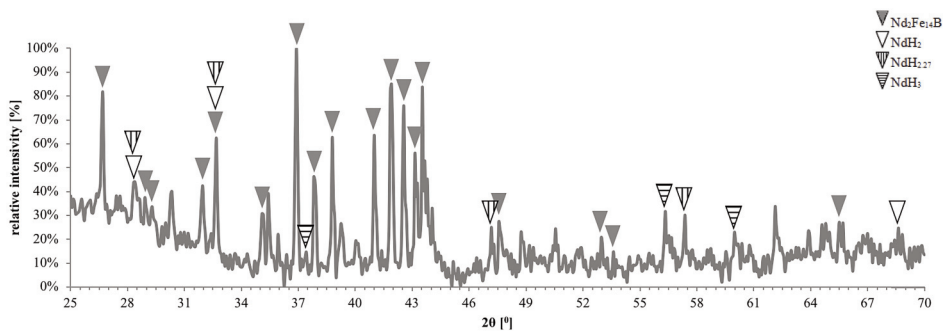


**Figure 16.** XRD patterns of sample obtained at room temperature and 4 bar



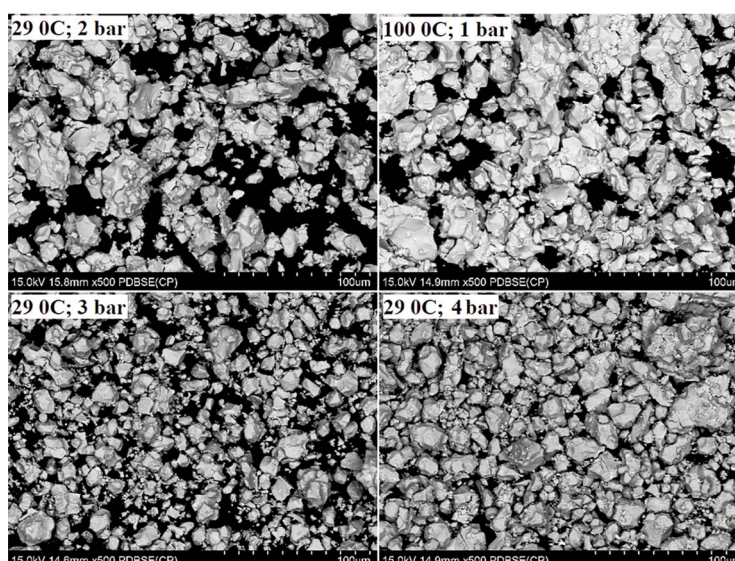


Figure 18. SEM images of sieved materials

#### 4. Conclusions

Complete disintegration of neodymium magnets under hydrogen atmosphere occurred at a relatively low temperature ( $<100\text{ }^{\circ}\text{C}$ ) and high pressure (2-4 bar). Hydrogen uptake increased with increasing pressure and decreases with increasing temperature. Increased pressure and temperature reduced the process duration.

During the HD process, a number of phase transformations occurred in neodymium magnets. The characteristic areas in material were formed at the grain boundaries (“necks”) and triple points (“pools”) resulting from synthesizing neodymium hydrides. XRD analyzes showed that the presence of neodymium hydrides was recorded in each case, regardless of the process parameters.

The decrepitation process can be used as a method of separating the magnet from the protective coating, which was a contaminant. High pressure during HD process was not recommended when using a sieving method for coating separation, so the best conditions for decrepitation, in this regard, according to the above tests; were a temperature  $29\text{-}100\text{ }^{\circ}\text{C}$  and pressure 1-2 bar.

The choice of technological parameters is a compromise between, the extent of disintegration, the process duration, and the size and number of pieces of coating, which can be easily and efficiently separated by sieving.

#### References

- [1] M. Firdaus, M.A. Rhamdhani, Y. Durandet, W.J. Rankin, K. McGregor, J. Sustain. Metall., 2 (2016) 276-295.
- [2] J. Jacobson, A. Kim, J. Appl. Phys., 61 (8) (1987) 3763-3765.
- [3] Y. Li, H.E. Evans, I.R. Harris, I.P. Jones, Oxid. Met., 59 (1) (2003) 167-182.
- [4] T. Uda, Mater. Trans., 43 (1) (2002) 55-62.
- [5] M. Itoh, K. Miura, K. Machida, J. Alloys Compd., 477 (2009) 484-487.
- [6] T.H. Okabe, O. Takeda, K. Fukuda, Y. Umetsu, Mater. Trans., 44 (4) (2003) 798-801.
- [7] X.T. Li, M. Yue et al., J. Alloys Compd., 649 (2015) 656-660.
- [8] T. Oishi, H. Konishi, T. Nohira, M. Tanaka, T. Usui, Kagaku Kogaku Ronbunshu, 36 (4) (2010) 299-303.
- [9] A.M. Martinez, O. Kjos, E. Skybakmoen, A. Solheim, G.M. Haarberg, ECS Trans., 50 (11) (2012) 453-461.
- [10] H. Konishi, H. Ono, E. Takeuchi, T. Nohira, T. Oishi, ECS Trans., 64 (4) (2014) 593-600.
- [11] Z. Hua, J. Wang et al., ACS Sustain. Chem. Eng., 2 (11) (2014) 2536-2543.
- [12] M. Yue, X. Yin et al., ACS Sustain. Chem. Eng., 6 (5) (2018) 6547-6553.
- [13] M. Zakotnik, I.R. Harris, A.J. Williams, J. Alloys Compd., 450 (2008) 525-531.
- [14] M. Zakotnik, I.R. Harris, A.J. Williams, J. Alloys Compd., 469 (1-2) (2009) 314-32.
- [15] Walton, H. Yi et al., J. Clean. Prod., 104 (2015) 236-241.
- [16] E.H. Lalana E. H.; School of Metallurgy and Materials, College of Engineering and Physical Sciences, University of Birmingham (2016) 1-313.
- [17] R.S. Sheridan, I.R. Harris, A. Walton, J. Magn. Mater., 401 (2016) 455-462.
- [18] Y. Kataoka, Y. Kawamoto, T. Ono, M. Tsubota, J. Kitagawa, Results Phys., 5 (2019) 99-100.
- [19] M. Awais, F. Coelho, M. Degri, E. Herraiz, A. Walton, N. Rowson, Recycling, 2 (4) 22 (2017) 1-11.
- [20] Y. Yang, A. Walton et al., J. Sustain. Metall., 3 (2017) 122-149.
- [21] M. Yue, X. Yin, W. Liu, Q. Lu, Chin. Phys., 28 (7) B (2019) 1-11.



## KORIŠĆENJE POSTUPKA DEKREPITACIJE U PRISUSTVU VODONIKA ZA RECIKLIRANJE Nd-Fe-B MAGNETA IZ ELEKTRONSKOG OTPADA

A. Piotrowicz <sup>a,\*</sup>, S. Pietrzyk <sup>b</sup>, P. Noga <sup>a</sup>, L. Myćka <sup>a</sup>

<sup>a</sup> AGH univerzitet za nauku i tehnologiju, Fakultet za obojene metale, Krakov, Poljska

<sup>b</sup> Istraživačka mreža Łukasiewicz, Institut za obojene metale, Gliwice, Poljska

### Apstrakt

*Ključni elementi u proizvodnji NdFeB magneta su elementi retke zemlje kao što je neodijum. Snabdevanje ovim elementom je imalo značajne nedostatke u nedavnoj prošlosti. Recikliranje NdFeB magneta koji se nalaze u elektronskom otpadu može da obezbedi alternativno snabdevanje ovim materijalima. Različiti postupci reciklaže za dobijanje sinterovanih NdFeB magneta su ispitivani. Dekrepitacija u prisustvu vodonika se može koristiti kao postupak za direktnu ponovnu upotrebu i kao efikasna metoda za reciklažu gde se čvrsti sinterovani magneti pretvaraju u demagnetizovani prah koji se koristi za dalju obradu. U ovom radu je predstavljena primena postupka dekrepitacije u prisustvu vodonika na sinterovane Nd-Fe-B magnete bez prethodnog uklanjanja metalnog zaštitnog sloja. Analizator gasne sorpcije je korišćen za određivanje količine apsorbovanog vodonika u uzorcima magneta pod kontrolisanim pritiskom (1, 2, 3 i 4 bara) i temperaturom (sobna, 100, 300 i 400 °C) koristeći sivert volumetrijsku metodu. ICP, XRD i SEM-EDS analiza su korišćene za ispitivanje sastava i morfologije polaznih i dobijenih materijala.*

**Ključne reči:** Neodijumski magneti; Reciklaža NdFeB; Postupak dekrepitacije u prisustvu vodonika

